JOURNAL OF STRUCTURAL INTEGRITY AND MAINTENANCE
https://doi.org/10.1080/24705314.2023.2170620

Taylor & Francis
Taylor & Francis Group

Interfacial bond strength of coloured SCC repair layers: an experimental and optimisation study

Oveys Ghodousian[a], Reyes Garcia[b], Vahid Shafaie[c] and Amin Ghodousian[b,d]

[a]Department of Civil Engineering, Islamic Azad University, Takestan, Iran; [b]Civil & Environmental Engineering Stream, School of Engineering, The University of Warwick, Coventry, UK; [c]Department of Structural and Geotechnical Engineering, Széchenyi István University, Győr, Hungary; [d]Department of Engineering Science, University of Tehran, Tehran, Iran

ABSTRACT

This study investigates experimentally and analytically the interfacial bond strength of coloured SCC repair layers. Ten SCC mixes with 5%, 10% and 15% of blue, green or red pigments were produced to examine their fresh properties. Subsequently, 60 coloured SCC specimens were tested to assess interfacial bond strength using pull-off and push-out tests. The results confirm that pigments reduce the mechanical properties of SCC and its bond strength to concrete substrates, with red pigment reducing (by up to 41%) interfacial bond strength. It is shown that the push-out test is effective to determine the interfacial shear bond strength between the SCC repair layers and substrates. A GNNC-Modified PSO algorithm is proposed to calculate accurately ($R^2 = 0.95$) the interfacial bond strength of coloured SCC repair layers. This study contributes towards developing more effective test methods and more accurate models to calculate interfacial bond strength of the SCC repair layers used in this study.

KEYWORDS

Self-compacting concrete; interfacial bond strength; push-out tests; GNNC-modified PSO algorithm; concrete repairs

Introduction

Screeding and concrete base repairs are widely used to extend the life of concrete floors and slabs that have experienced aging or structural damage (Chen et al., 1995; Espeche & León, 2011). In these repairs, a cementitious (repair) layer is typically laid onto an existing concrete layer (substrate) to make them work as a "single" slab unit. The structural integrity of the repair layer relies heavily on the mechanical bond mobilised at the interface between the repair and substrate layers. The strength of such interfacial bond is affected by the properties of the concrete substrate and repair layer, type and level of consolidation, shrinkage, environmental conditions, among others (Courard et al., 2014). Ensuring proper bond between a new repair layer and the existing concrete substrate is therefore critical in the repair of concrete structures (Emmons & Vaysburd, 1994; Morgan, 1996). Whilst many materials exist to repair concrete structures (e.g. polymeric or resin materials, polymer-modified cementitious materials, etc). (Lukovic et al., 2012; Morgan, 1996; Qian et al., 2014)), cement-based concrete is still extensively used because i) its mechanical characteristics are often similar to those of existing concrete substrate layers, and ii) concrete has proven to be a cost-effective solution in the construction industry.

Previous studies have confirmed that poor interfacial bond can lead to structural issues in concrete repairs (Beaupré, 1999; Bonaldo et al., 2005; Momayez et al., 2005; Mu et al., 2002), particularly at the interface between the repair and substrate layers. Different techniques have been proposed to improve the interfacial bond strength and to measure the effectiveness of the repairs via bond strength tests. For instance, Courard et al. (2014) used pull-off cohesion tests to examine the effect of preparing (roughening) the surface of the concrete substrate. Wang et al. (2016) performed pull-off tests to evaluate the tensile bond strength between ultra-high toughness cementitious composites and existing concrete. Zanotti et al. (2018) used the slant-shear bond test to study the shear bond strength of fibre-reinforced mortar repair layers. It was reported that adding steel fibres increased the bonding of the repair layers to the substrates. Naderi and Ghodousian (2012) studied the bonding of self-compacting repair overlays on different concrete substrates. They also assessed the bond strength at the substrate-repair layer interface using friction transfer or twist-off tests, and found the former test to be more suitable to assess interfacial bond. The results in Naderi and Ghodousian also showed that dry and saturated wet surfaces led to low bond strengths between the repair layer and substrate, whereas applying cement grout to the substrate significantly increased the bond strength. Momayez et al. (2005) compared four different tests to determine bond strength between two concretes: pull-off, slant shear, splitting prisms and direct shear (bi-surface) tests. Momayez et al. found that the experimental value of bond strength depended on the test type, according to this descending order: slant shear, bi-surface shear, splitting, and pull-off test. Guo et al. (2018) measured the bond strength of a new concrete for rapid patch repairs of pavements using splitting tensile tests and direct shear tests. The results from the direct shear strength tests found that the bond strength of high surface roughness specimens reduced to 66.3% of its original value. Gadri & Guettala (2017) conducted flexure and splitting tests in order to assess the bond strength of composite specimens. The results indicated that sand concrete had a good bond strength, thus proving to be a suitable cementitious repair material.

More recently, Rashid et al. (2020) assessed the bond strength between four different adhesive overlays including cement paste, epoxy bonding agent, styrene butadiene rubber (SBR)-latex, and Carbon Fibre Reinforced Polymers (CFRPs). They found that CFRPs had the highest bond

CONTACT Reyes Garcia reyes.garcia@warwick.ac.uk

strength, whereas the cement paste had the lowest bond strength. Ganesh et al. (Ganesh & Ramachandra Murthy, 2020) used a numerical approach to calculate the bond strength between normal strength concrete (NSC) and ultra-high-performance concrete (UHPFRC) through different tests (slant shear, split tensile and four-point bending). Ganesh et al. also modelled the bond strength numerically and matched reasonably well their experimental results, with maximum differences of 12%. Mansour & Fayed (2021) studied the effect of interfacial surface preparation on bond strength of normal and UHPFRC repairs. The results showed that UHPFRC had better overall interfacial performance than NSC, mainly because the viscosity of UHPFRC repairs effectively filled the pores of the substrate. Luo et al. (2021) performed a FE analysis to optimise the bond strength at the interface of concrete repairs using grooves on the substrate surface. They found that the strength at the interfacial transition zone (ITZ) played an important role in enhancing the chemical adhesive force. Despite the numerous studies, to date no consensus exist on the most suitable type of test to assess the interfacial bond strength mobilised between repair layers. Some of the above tests require special equipment or can lead to doubtful results as failure does not always occur at the interface of the repair layer. However, compared to other test methods, splitting and push-out tests are deemed to be more suitable to assess the interfacial bond strength because failure always occurs at the interface between the repair and substrate layers.

Very often, the vibration/consolidation necessary to achieve a proper bond at the repair layers can be difficult and time-consuming, which in turn increases repair costs. To bypass this issue, self-compacting concrete (SCC) can be used to improve interfacial bond. In many cases, the aesthetic appearance of the repair layer is also enhanced by adding colour pigments into the concrete mix. Whilst some studies have investigated the use of pigments in mortars (Zurita Ares et al., 2014) and normal concrete (Naderi et al., 2012), very limited research exists on coloured SCC mixes. In one of such few studies, López et al. (2009) proposed a mortar-based design for coloured SCC that leads to a rapid and easy optimisation of mix proportions. More recently, Ghalehnovi et al. (2019) found that the addition of red mud in SCC affected the rheological and mechanical properties of SCC but only marginally (less than 5%). However, the addition or red mud improved the durability of SCC to sulphate attack. More recent studies have examined aggregate bulking and water thickness in cement-base composites (Li et al., 2022; Qiu et al., 2020). Due to the lack of studies, further research is deemed necessary to investigate the full potential of coloured SCC repair layers in construction. It should be noted that one of the main advantages of adding colour pigments directly into concrete is that the colour extends uniformly throughout the concrete. Moreover, the colour is expected to remain unchanged even if the concrete is exposed to abrasion, weathering or ultraviolet light. Adding pigments is also convenient as this could lead to labour savings. Firstly, because the colour pigments are incorporated in the concrete, and thus placing and finishing of the concrete can be performed as usual. Secondly, because unlike other colouring methods (e.g. coloured surface coatings), there is no need for recolouring or recoating the concrete surface after years of service.

The calculation of bond strength at the interface of two concrete layers is challenging due to the high (tensile) variability of concrete, lack of uniformity in testing procedures, lack of test data, and difficulty of measuring the actual bond strength being mobilised at the interface. This is reflected on the limited predictive models available in the literature (Ganesh & Ramachandra Murthy, 2020). In the last 20 years, neural networks have been widely used to develop models that predict the compressive strength of concrete (Alshihri et al., 2009; Zarandi et al., 2008; Imam et al., 2021; Jiang, 2012; Mohamed et al., 2021; Muthupriya et al., 2011; Sharma et al., 2020; Öztaş et al., 2006). Unlike other mathematical methods (e.g. linear regression), artificial neural networks (ANNs) have proven suitable to predict bond properties. For instance, Naderi and Ghodousian (2012) successfully used fuzzy logic methods to predict the bond strength between two concrete layers. Milovancevic et al. (2021) used adaptive neuro fuzzy inference systems (ANFIS) to predict the shear bond strength of concrete structures with high-performance fibre-reinforced concrete. To date however, the use of ANN in the prediction of interfacial bond strength is still limited.

This article examines experimentally and analytically the interfacial bond strength of coloured SCC repair layers. To achieve this, the fresh properties of ten coloured SCC mixes with 5%, 10% and 15% of blue, green or red pigments (added as weight percentage of cement plus fly ash) are first examined. Afterwards, 60 coloured SCC specimens were tested to assess their interfacial bond strength using pull-off and push-out tests. Based on the test results from the pull-off tests, a nearest neighbourhood clustering (GNNC)-modified PSO algorithm (Ghodousian et al., 2021) is used to propose a new approach to calculate interfacial bond strength in an accurate way. The results of this study contribute towards better testing methods to assess the interfacial bond strength of SCC repair layers, as well as towards more accurate techniques to calculate interfacial bond strength. Specifically, this study provides new experimental data on the bond strength between coloured SCC repair layers and the concrete substrate, mainly because such data do not exist in the current literature. Moreover, the bond strength between coloured SCC repair layers and the concrete substrate is modelled using the GNNC-modified PSO algorithm, which is completely new application of this type of mathematical approach.

Experimental programme

Mix design and material properties

Table 1 summarises the mix proportions of the ten mixes used as repair overlays. Mix 1 (Fa10) was a control mix without any pigments. Mixes 2 to 10 had pigments (green, red or blue) at levels of 5%, 10% or 15% of replacement by weight of combined cement and fly ash. A maximum replacement level of 15% was chosen because adding 20% pigments reduced considerably the fresh properties of the mixes, as explained later. Table 2 lists the characteristics of the (white) cement used in the mixes, whereas Table 3 describes the properties of the three pigments. All mixes were produced with fluvial rounded sand with a unit weight of 2.6 g/cm^3 and a water absorption of 2.5%. Likewise, riverbed gravel with a maximum size of 12.5 mm and a unit weight of 2.64 g/cm^3 was used in

Table 1. Mix proportions of SCC repair layers.

No	Mix ID	C kg/m^3	FA kg/m^3	LS kg/m^3	S kg/m^3	G kg/m^3	W kg/m^3	w/c -	P kg/m^3	SP %
1	Fa10	405.00	45	211.00	790	800	157.5	0.35	0.0	0.9
2	Blue5	402.83	44.76	209.87	785.77	795.71	157.5	0.35	22.5	0.9
3	Green5	403.14	44.79	210.03	786.37	796.33	157.5	0.35	22.5	0.9
4	Red5	403.10	44.79	210.01	786.30	796.25	157.5	0.35	22.5	0.9
5	Blue10	400.66	44.52	208.74	781.54	791.43	157.5	0.35	45.0	0.9
6	Green10	401.28	44.59	209.06	782.75	792.65	157.5	0.35	45.0	0.9
7	Red10	401.20	44.58	209.02	782.59	792.50	157.5	0.35	45.0	0.9
8	Blue15	398.49	44.28	207.61	777.30	787.14	157.5	0.35	67.5	0.9
9	Green15	399.42	44.38	208.09	779.12	788.98	157.5	0.35	67.5	0.9
10	Red15	399.31	44.37	208.03	778.89	788.75	157.5	0.35	67.5	0.9

C: White Cement; FA: Fly Ash; LS: Limestone Powder; S: Sand; G: Gravel; W: Water; P: Pigment; SP: Superplasticiser.

Table 2. Properties of white cement used in the SCC mixes.

Whiteness		Blaine Value (cm^2/g)	Initial setting time (min)	Final setting time (min)	Autoclave expansion (%)	28-day compressive strength (MPa)
Y-Value	W					
79.5	90.5	3520	140	210	0.1	22.5
Sio_2 (%)	Al_2O_3 (%)	Fe_2O_3 (%)	CaO (%)	MgO (%)	SO_3 (%)	
22.7	4.1	6.3	66.7	0.9	2.7	

Table 3. Properties of pigments used in the SCC mixes.

Colour	Fe_2O_3 (%)	SiO_2 (%)	Cr_2O_3 (%)	Density (g/cm^3)	PH	Moisture (%)	Particle shape	Particle size (μm)
Green	5 - 50	-	25 - 75	4.9	5 - 7	>1.5	Round	0.4–0.5
Red	96	1	-	4.8	3 - 7	>1.0	Round	0.15–0.25
Blue	85	-	-	4.2	5 - 6	>0.5	Round	0.20–0.30

the mixes. Figures 1(a) and 1(b) show, respectively, the grading curves of the fine and course aggregates according to ASTM C33 (2018). The fly ash used in the mixes had a specific surface area of 4000 cm^2/g, and a unit weight of 2.5 g/cm^3. It should be mentioned that segregation resistance is an important parameter in SCC. Therefore, the authors performed a series of preliminary trail mixes to develop SCC mix designs without segregation. Accordingly, none of the mix proportions summarised in Table 1 had visible signs of segregation.

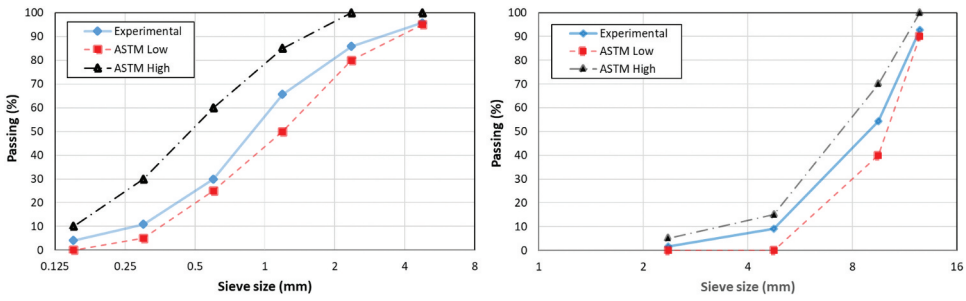

a) b)

Figure 1. Grading curves of (a) fine aggregate, and (b) coarse aggregate.

a) b) c)

Figure 2. View of typical: (a) slump flow test, (b) L-box test, and (c) V-funnel test.

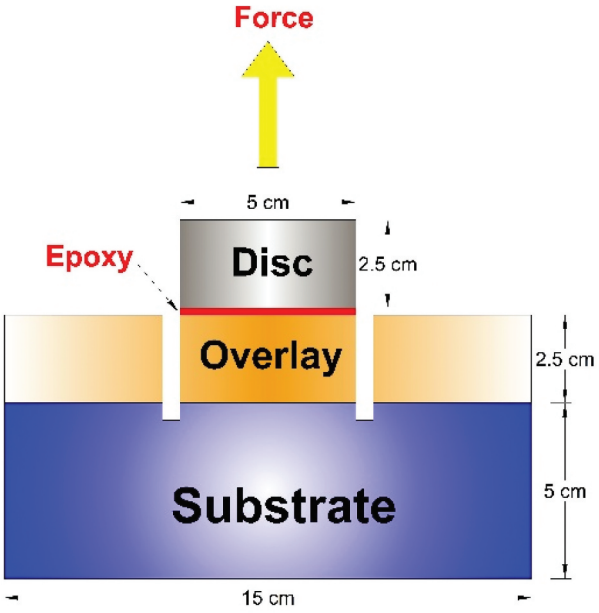

Figure 3. Schematic view of the half-core pull-off test.

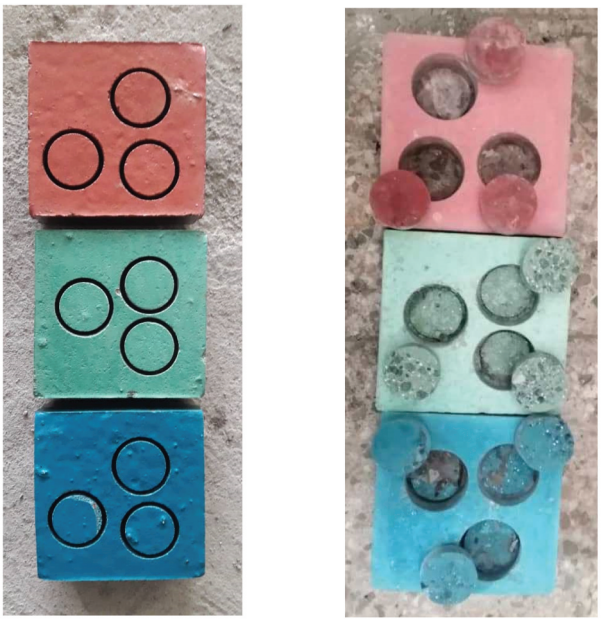

Figure 4. (a) View of pull-off specimens before applying the tensile force, and (b) Failure of coloured SCC repair layers from their concrete substrate.

The properties of the fresh mixes were investigated using:

- Slump flow tests, measured by the diameter of the circle (see Figure 2(a)),
- L-box tests (Figure 2(b)), measured by the blockage ratio, and
- V-funnel tests (Figure 2(c)), measured by the discharge time.

To examine the interfacial bond strength of the coloured SCC mixes, pull-off and push-out test specimens were also cast and subsequently tested, as described in the following sub-sections.

Pull-off specimens and testing

These specimens consisted of a 2.5 cm-thick repair layer cast over a concrete substrate block with dimensions 15 × 15 × 5 cm (see Figure 3). The substrate was cast six months before the actual test to avoid any shrinkage effects. After the repair layer was cured for 28 days, a 3 cm-thick half-coring was performed (i.e. the half-coring included the full thickness of the repair layer, plus 0.5 cm of substrate). After coring, the bond strength between the two layers was determined using a metal disc with a diameter of 5 cm, and a height of 2.5 cm according to ASTM C1583 (ASTM-C1583, 2014). The results

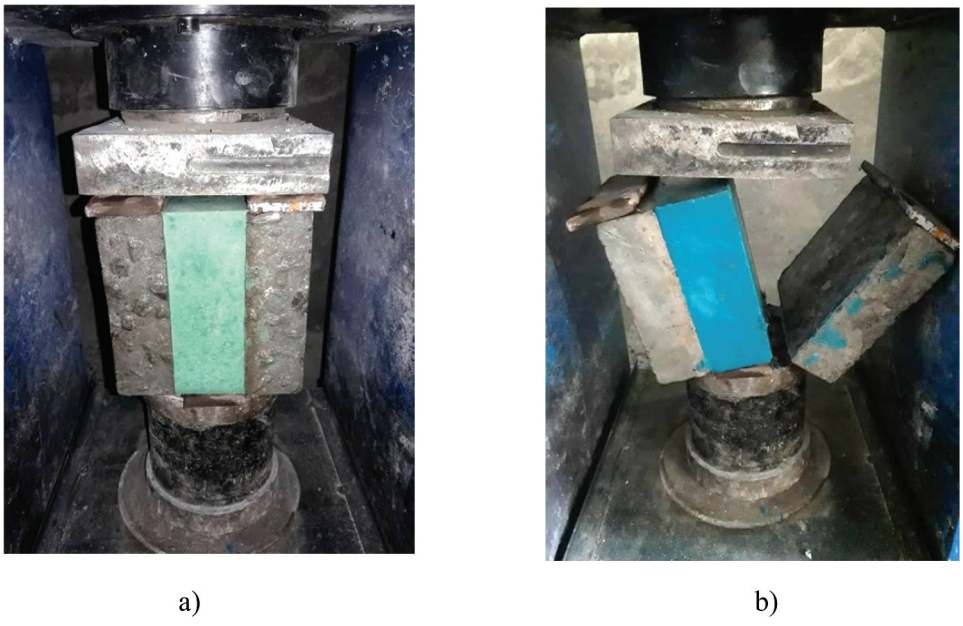

Figure 5. (a) View of push-out test setup and specimen, and (b) typical failure of specimens.

from the pull-off tests are reliable only if failure occurs at the interface between the repair layer and the substrate. For this reason, the results from specimens that failed at the epoxy adhesive (used to glue to the metal disc to the specimen), or within the repair layer and/or concrete substrate themselves are not presented in this study. Figures 4(a) and 4(b) show typical pull-off specimens before and after failure, respectively.

Push-out specimens and testing

The substrate of these specimens consisted of two 5 cm-thick concrete blocks cut out from cubes cast six months before the test. In between these two blocks, a 5 cm block was then cast with the coloured SCC mixes to produce a 15 cm cube. Accordingly, the coloured SCC repair layer was bonded to the substrate on two faces. In this test, failure typically occurs on the face with the lowest interfacial bond strength. Compared to the pull-off test, the push-out test is more practical because no special equipment is required (only a flat jack), and because failure always occurs at one of the interfaces, thus leading to more reliable results. Figure 5(a) shows the test setup, whereas Figure 5(b) shows a typical specimen after failure at one of the interfaces. It should be noted that, in both pull-off and push-out specimens, the concrete substrate was saturated surface dry (SSD) when the SCC repair layer was cast as this is the best condition to promote a better interfacial bond. To achieve such SSD conditions, the concrete substrates were fully submerged in water. After several days, the substrates were taken out of the water, and their surfaces were dried using an industrial drier just before applying the coloured SCC overlay.

Results and discussion

Fresh properties

Figures 6(a), 6(b) and 6(c) report the results from the V-funnel, L-box and slump flow tests, respectively. The results show that, compared to the control mix Fa10, the fresh properties of all coloured SCC mixes degraded consistently with increasing amounts of pigment. Overall, the blue pigment led to the lowest degradation in fresh properties, whereas the red pigment had the worst effect. For example, with increasing amounts of pigment, the discharging time of the V-funnel tests increased (Figure 6(a)), whereas the blockage ratio of the L-box tests reduced (Figure 6(b)). Similarly, a 5% of blue pigment reduced the slump flow diameter by 7% compared to mix Fa10 (Figure 6(c)), while this drop was 27% for a 15% of red pigment replacement.

The results in Figures 6(a), 6(b) and 6(c) also show that, according to the EFNARC (EFNARC, 2005) mix classification, the discharge time (V-funnel test) of mixes Fa10, Blue5, Green5, Red5, Blue10 and Green10 was below 8 s, which means these mixes are classified as VS1/VF1. However, mixes Red10, Blue15, Green15 and Red15 were classified as VS2/VF2 as their discharge time was between 9 and 25 s. Regarding the L-box results, most of the mixes (except Red15 and Green15) were classified as PA2, i.e. mixes with a blockage ratio >0.8. Likewise, the slump flow of mixes Red 10, Green 15, Blue 15, and Red 15 were classified as SF1 (550–650 mm) according to EFNARC, whereas mixes FA10, Blue5, Green5, Red5, Blue10 and Green10 were classified as SF2 (660–750 mm).

It should be also noted that the authors attempted SCC mixes with a 20% pigment replacement, but this led to a loss of the self-compacting properties of the concrete. Accordingly, a maximum pigment content of 15% was chosen in this study. After performing the tests on the fresh mixes, 15 cm cubes and standard cylinders (15 cm diameter and 30 cm height) were cast to carry out compressive and tensile tests, as described in the next section.

Compressive and tensile strengths and interfacial bond strength

Table 4 summarises the compressive (f_c) and tensile (f_{ctm}) strengths of the repair layers, as well as the interfacial bond strength from the pull-off and push-out specimens at 28 days. The table also shows the reduction rate (in %) of the above properties. Note that the results in Table 4 are the average of three specimens.

The results in Table 4 indicate that, compared to the control mix Fa10, the addition of pigments reduced the compressive strength of all coloured SCC mixes. The reduction in compressive strength was proportional to the amount of pigment, which explains why the highest compressive strength of all coloured SCCs is for a 5% replacement level (e.g. see mix Blue5). The results also indicate that the blue SCCs had the lowest decrease in compressive strength, whereas the red SCCs had the highest drop. Indeed, the

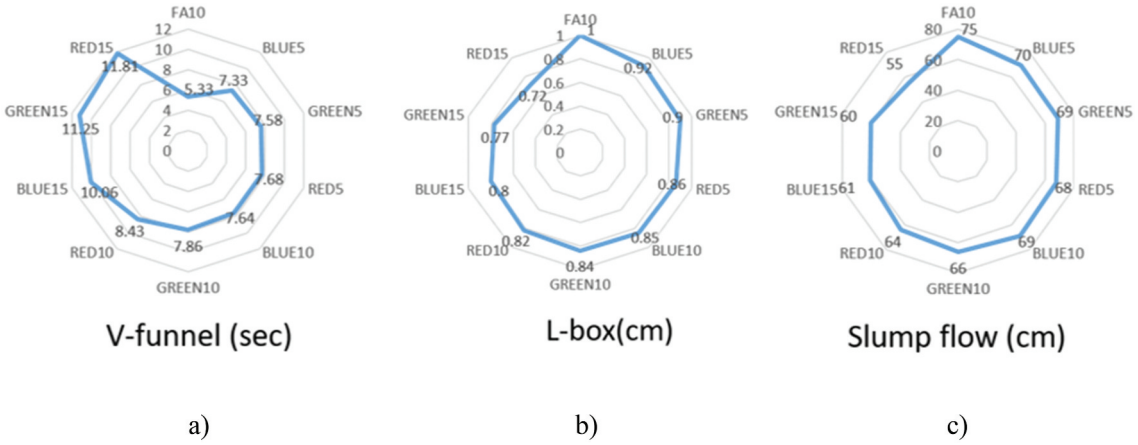

Figure 6. Fresh test results from coloured SCC mixes.

Table 4. Mechanical properties and interfacial bond strengths of tested specimens at 28 days.

				Interfacial bond strength (MPa)		Reduction rate (%)			
No.	Mix ID	f_{cm} (MPa)	f_{ctm} (MPa)	Pull-off test	Push-out test	f_{cm}	f_{ctm}	Pull-off test	Push-out test
1	Fa10	53.9	4.67	3.18	11.43	—	—	—	—
2	Blue5	49.6	4.24	2.79	10.86	8	9	12	5
3	Green5	46.7	4.09	2.58	9.99	13	12	19	13
4	Red5	37.5	3.42	2.39	8.07	30	27	25	29
5	Blue10	46.2	4.37	2.53	9.65	14	6	20	16
6	Green10	44.0	3.96	2.51	9.31	18	15	21	19
7	Red10	31.4	2.91	2.14	6.93	42	38	33	39
8	Blue15	41.6	3.57	2.34	8.98	23	24	26	21
9	Green15	38.6	3.51	2.19	8.21	28	25	31	28
10	Red15	30.0	2.70	1.87	6.15	44	42	41	46

addition of red pigment reduced more the compressive strength compared to blue and green pigments. For example, at a similar level of 10% replacement, the reductions in compressive strength of blue, green and red SCCs were −14% (mix Blue10), −18% (mix Green10) and −42% (mix Red10), respectively. The tensile strength of coloured SCCs followed a similar trend to that of the compressive strength.

The results from the pull-off bond tests listed in Table 4 indicate that, as expected, the control mix Fa10 had the highest interfacial bond strength. The bond strength consistently reduced as the amount of pigment increased. The lowest reduction in bond was for the SCC mix Blue5 with 5% of blue pigment (−12%), whereas the highest reduction was for the SCC mix Red15 with 15% of red pigment (−41%). Whilst pull-off tests provide the tensile interfacial bond strength, push-out tests measure shear debonding between two concrete layers. The push-out tests results indicate that the shear bond strengths between coloured SCC repair layers and the substrates are 3.2 to 3.9 times the tensile bond strengths obtained from the pull-off tests.

Figure 7 shows the relationship of the interfacial bond strengths obtained from the pull-off and push-out tests. The results in the figure show a clear trend between the results from both tests, with a high correlation coefficient of $R^2 = 0.9$. This suggests that the push-out test can be confidently used to determine the bond strength of two concrete layers. Compared to the pull-off test, the push-out test is also more convenient since it always provides usable results as failure always occurs at the weakest interface. It should be noted that, strictly speaking, pull-off tests measure the tensile bond strength at the interface, whereas the push-out test measures the shear bond strength. However, the results in Figure 7 confirm that there is a strong correlation between these two test results.

Figure 8 shows the relationship between the bond strength obtained from pull-off tests and the slump flow results of the ten coloured SCC mixes examined in this study. The trend of results suggests that there is a clear link between these two variables, as indicated by a relatively high correlation coefficient of $R^2 = 0.85$. This also suggests that slump flow results could be used to predict the bond strength between coloured SCC and the concrete substrate.

In the following section, the test results from the pull-off test are used to perform analyses using an innovative GNNC-modified PSO algorithm. Based on this, a new approach to calculate interfacial bond strength between SCC repair layers and a concrete substrate is also proposed.

A new GNNC-modified PSO algorithm to calculate interfacial bond strength of SCC repair layers

The results presented in previous sections are used here to establish relationships between the interfacial bond strength (*BS*), the slump flow (*SF*) and compressive strength (*CS*) test results. There parameters are deemed as representative of the fresh properties and hardened mechanical characteristics of the coloured SCC mixes. Whilst the bond strength at the interface of concrete repairs is often associated to the concrete tensile strength, the concrete compressive strength is used in this study because i) there is a strong correlation between these two concrete properties, and ii) the concrete tensile strength is not always obtained in real on-site applications. Moreover, the use of slump flow results in the calculations is also convenient because a) there is a correlation between the pull-off bond strength and the slump flow (as shown in Figure 8), and b) such value can be easily measured with standard testing equipment.

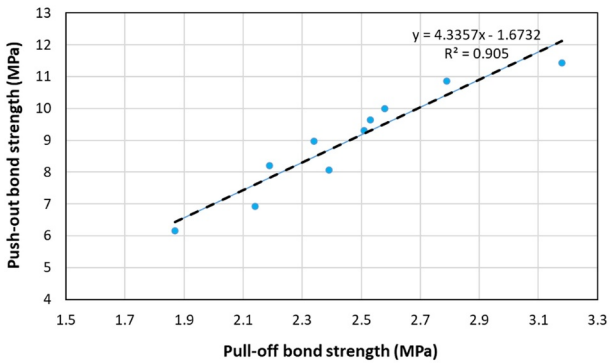

Figure 7. Relationship of interfacial bond strengths from pull-off and push-out tests.

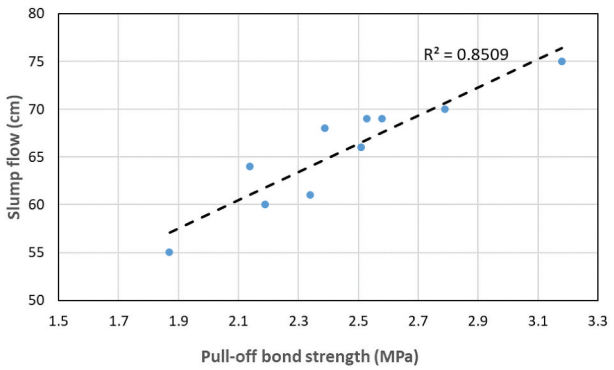

Figure 8. Relationship between interfacial pull-off bond strengths and slump flow test results.

Unlike heuristic methods (such as artificial neural networks) where a large amount of data is often needed to develop reliable models, the new GNNC-Modified PSO algorithm proposed in this study is based on a fuzzy logic approach that requires only a small number of data points. The fuzzy system is the most important part of the proposed algorithm, which is defined based on a finite number of *If-Then* fuzzy rules to generate practical functions approximating a set of input-output pairs. Although a large amount of data points may increase the accuracy of the results, this also increases the complexity of the algorithm and the computational time. In addition, the lack of data in fuzzy systems is compensated (to some extent) by the completeness property. This is done by membership functions defined in fuzzy systems, by which the data space is covered. More precisely, a point that is very far from the input-output data can be considered (probably with a very small membership function value) in the set of *If-Then* fuzzy rules. However, a reasonable minimum amount of data with a proper dispersion in the answer space is always needed, as it is the case in this study.

To assess the effectiveness of the proposed algorithm, a linear regression analysis is also carried out to provide a benchmark comparison between the two mathematical methods.

Linear regression analysis

A linear regression analysis was carried out to obtain Equation (1) with an $R^2 = 0.87$. Note that the regression analysis used all the experimental data of the pull-off tests (30 specimens) and not only the average values.

$$BS = -0.361 + 0.023(CS) + 0.028(SF) \quad (1)$$

In the above equation, the compressive and bond strengths are in MPa, and the flow test results are in cm. It should be mentioned that Equation (1) was obtained using the test results presented in this article and it should not be taken as a general equation applicable to other mixes different to the ones included here.

Proposed GNNC-modified PSO algorithm

A Generalised Nearest Neighbourhood Clustering (GNNC) method was also used to calculate the interfacial bond strength of the specimens. A modified Particle Swarm Optimisation (PSO) algorithm was also used to optimise the parameters of the fuzzy system by movements in a search space, including both continuous and integer variables. Figure 9 shows the main steps of the algorithm, which was implemented in MATLAB® software. Further details of the method are provided in Appendix A and only the main steps are listed below:

(1) Generate initial particles $X_p = [\sigma_{p1}, \sigma_{p2}, \ldots, \sigma_{pn}, r_p]$ $(1 \le p \le N)$, with random parameters $0 \le \sigma_{pj} \le 5 (1 \le j \le n)$ and $r_p \in \{d_0, 2d_0, \ldots, rd_0\}$.
(2) For each particle X_p $(1 \le p \le N)$, build its associated clusters with a radius r_p.
(3) For each particle X_p $(1 \le p \le N)$, use the resulting clusters and parameters $\sigma_{p1}, \sigma_{p2}, \ldots, \sigma_{pn}$ to design its associated optimum fuzzy system (see Equation (3) in Appendix A).
(4) Evaluate the fitness for each particle X_p $(1 \le p \le N)$ using Equation (4) in Appendix A.
(5) Check if at least one of the terminating criteria (Equation (6) in Appendix A) is satisfied, then move on to Step 7.
(6) Update X_p and V_p by the modified Equation (5), and then move on to Step 2.
(7) Return the optimal approximator.

In this study, the input variables are the compressive strength (*CS*) and slump flow table diameter (*SF*), whereas the output variable is the interfacial bond strength (*BS*). It should be noted that 70% of the specimens (21 specimens) were selected randomly as training data, whereas the remaining specimens were used as test data. The membership functions were assumed to be Gaussian functions. In the GNNC-modified PSO algorithm, the swarm size was set to 50 and the number of iterations was chosen to be 20.

Figure 10 shows the relationship between the predicted and measured interfacial bond strength for all data. The

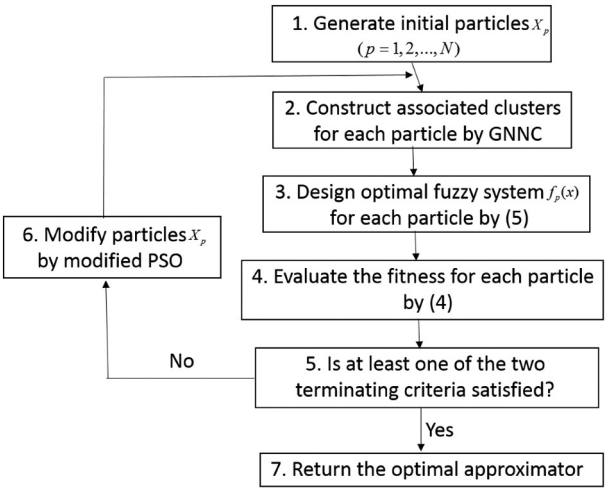

Figure 9. General steps of GNNC-modified PSO algorithm.

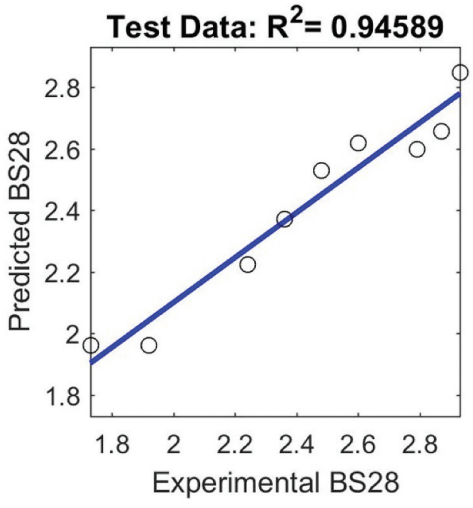

Figure 10. Relationship between experimental and predicted pull-off bond strength using the GNNC-Modified PSO algorithm.

optimal solution resulted from the GNNC-modified algorithm with the following settings:

$$OptimalSolution = [1\ ,\ 1\ ,\ 1.1007]$$
$$\sigma_1^* = 1$$
$$\sigma_2^* = 1$$
$$r^* = 1.1007$$
$$Number\ of\ Clusters = 18$$

The results in Figure 10 show that the GNNC-Modified PSO algorithm can predict interfacial bond strength more accurately ($R^2 = 0.95$) than the linear regression method ($R^2 = 0.87$). Based on the results of this study, it is possible to conclude that GNNC-modified PSO algorithm is a suitable approach to predict interfacial bond strength between SCC repair layers and concrete substrates. However, since the experimental database used to train the algorithm was relatively small, further experimental research is necessary to obtain more results and verify the applicability of the algorithm to other types of coloured SCC concrete repairs.

Moreover, whilst this study examined the bond strength between coloured SCC repair layers and concrete substrates, the bond behaviour between two concrete layers is a complex phenomenon that can be affected by other factors such as the strength of the weakest concrete surface, interfacial roughness, soundness and cleanliness of the surfaces, moisture condition of substrate, age of substrate, position of the interface, use of interfacial bonding agent, type/quality workmanship, and curing conditions, among others. Consequently, more research is necessary to quantify the effect of the above factors so as to develop more comprehensive interfacial bond strength models for SCC repair layers. The examination of the microstructure at the interface (e.g. using SEM images) is also necessary to explain how the pigments influence bonding between the coloured SCC and the substrate. Other aspects such the effect of the particle size of pigments (which influences the packing system and water film thickness and thus the fluidity of SCC) should be also considered in future experimental research.

Summary and conclusions

This article investigated experimentally and analytically the interfacial bond strength of coloured Self-Consolidating Concrete (SCC) repair layers on concrete substrates. Ten SCC mixes with 5%, 10% and 15% of blue, green or red pigments used as cement and fly ash replacement were produced to examine their fresh properties and to assess interfacial bond strength using pull-off and push-out tests. Using these test results, a new GNNC-Modified PSO algorithm was proposed to calculate the interfacial bond strength of coloured SCC repairs. Based on the results of this study, the following conclusions are drawn:

- The presence of pigments reduced the fresh properties of coloured SCC mixes. Overall, the blue pigment led to the lowest reductions, whereas the red pigment had the worst effect. For example, replacing a 15% of red pigment reduced the slump flow table results by 27% compared to the control mix.
- The pigments also reduced the compressive and tensile strength of all SCCs, and such reductions were proportional to the amount of pigment replacement. At a similar level of 10% cement and fly ash replacement, the reductions in compressive strength of blue, green and red SCCs were 14%, 18% and 42%, respectively.
- The results from the pull-off bond tests showed that the interfacial bond strength of SCC repairs consistently reduced with the amount of pigment replacement. The highest reduction of interfacial bond strength (up to 41%) was for a SCC with 15% of red pigment.
- Compared to other test setups proposed in the technical literature, push-out tests can be suitable to assess interfacial bond strength because no special equipment is required and because failure always occurs at one interface of the repair layers, thus leading to more useful and reliable results. Therefore, it is proposed to adopt this test setup in future studies examining interfacial bond strength of concrete repairs.
- The proposed GNNC-Modified PSO algorithm calculates accurately ($R^2 = 0.95$) the interfacial bond strength of coloured SCC repairs over concrete substrates. However, future research should extend the experimental database used to train the algorithm. More research is also necessary to extend the application of the proposed algorithm to other types of SCC mixes. Other factors that should be investigated include the strength of the concrete substrate surface, interfacial roughness, soundness and cleanliness of the surfaces, moisture condition of substrate, age of substrate, position of the interface, use of interfacial bonding agent, type/quality workmanship, and curing conditions, among others.

Disclosure statement

No potential conflict of interest was reported by the author(s).

References

Alshihri, M. M., Azmy, A. M., & El-Bisy, M. S. (2009). Neural networks for predicting compressive strength of structural light weight concrete. *Construction and Building Materials*, *23*(6), 2214–2219. https://doi.org/10.1016/j.conbuildmat.2008.12.003

ASTM-C1583. (2014). *Standard test method for tensile strength of concrete surfaces and the bond strength or tensile strength of concrete repair and overlay materials by direct tension (pull-off method)*, *ASTM International*. https://doi.org/10.1520/C1583

ASTM C33/C33M-18. (2018). *Standard specification for concrete aggregates*, *astm international*. https://doi.org/10.1520/C0033_C0033M-18

Beaupré, D. (1999). Bond strength of shotcrete repair. *Shotcrete Magazine*, 12–15. http://www.shotcrete.org/pdf_files/Sp99Beaupre.pdf.

Bonaldo, E., Barros, J. A. O., & Lourenço, P. B. (2005). Bond characterization between concrete substrate and repairing SFRC using pull-off testing. *International Journal of Adhesion and Adhesives*, *25*(6), 463–474. https://doi.org/10.1016/j.ijadhadh.2005.01.002

Chen, P. W., Fu, X., & Chung, D. D. L. (1995). Improving the bonding between old and new concrete by adding carbon fibers to the new concrete. *Cement and Concrete Research*, *25*(3), 491–496. https://doi.org/10.1016/0008-8846(95)00037-D

Courard, L., Piotrowski, T., & Garbacz, A. (2014). Near-to-surface properties affecting bond strength in concrete repair. *Cement and Concrete Composites*, *46*, 73–80. https://doi.org/10.1016/j.cemconcomp.2013.11.005

EFNARC. (2005). *The European guidelines for self-compacting concrete-Specification, Production and Use*. International Bureau for Precast Concrete (BIBM), Brussels, Belgium.

Emmons, P. H., & Vaysburd, A. M. (1994). Factors affecting the durability of concrete repair: The contractor's viewpoint. *Construction and Building Materials*, *8*(1), 5–16. https://doi.org/10.1016/0950-0618(94)90003-5

Espeche, A. D., & León, J. (2011). Estimation of bond strength envelopes for old-to-new concrete interfaces based on a cylinder splitting test.

Construction and Building Materials, *25*(3), 1222–1235. https://doi.org/10.1016/j.conbuildmat.2010.09.032

Gadri, K., & Guettala, A. (2017). Evaluation of bond strength between sand concrete as new repair material and ordinary concrete substrate (The surface roughness effect). *Construction and Building Materials*, *157*, 1133–1144. https://doi.org/10.1016/j.conbuildmat.2017.09.183

Ganesh, P., & Ramachandra Murthy, A. (2020). Simulation of surface preparations to predict the bond behaviour between normal strength concrete and ultra-high performance concrete. *Construction and Building Materials*, *250*, 118871. https://doi.org/10.1016/J.CONBUILDMAT.2020.118871

Ghalehnovi, M., Shamsabadi, E. A., Khodabakhshian, A., Sourmeh, F., & De Brito, J. (2019). Self-compacting architectural concrete production using red mud. *Construction and Building Materials*, *226*, 418–427. https://doi.org/10.1016/J.CONBUILDMAT.2019.07.248

Ghodousian, O., Behdad, K., Shafaie, V., Ghodousian, A., & Mehdikhani, H. (2021). Predicting 28-day compressive strength of pozzolanic concrete by generalized nearest neighborhood clustering using modified pso algorithm. *Malaysian Construction Research Journal*, *33*(1), 61–72.

Guo, T., Xie, Y., & Weng, X. (2018). Evaluation of the bond strength of a novel concrete for rapid patch repair of pavements. *Construction and Building Materials*, *186*, 790–800. https://doi.org/10.1016/j.conbuildmat.2018.08.007

Imam, A., Salami, B. A., & Oyehan, T. A. (2021). Predicting the compressive strength of a quaternary blend concrete using bayesian regularized neural network. *Journal of Structural Integrity and Maintenance*, *6*(4), 237–246. https://doi.org/10.1080/24705314.2021.1892572

Jiang, J. (2012). Prediction of concrete strength based on BP neural network. *Advanced Materials Research*, *341–342*, 58–62. https://doi.org/10.4028/www.scientific.net/AMR.341-342.58

Li, L. G., Feng, J. J., Lu, Z. C., Xie, H. Z., Xiao, B. F., Kwan, A. K. H., & Jiao, C. J. (2022). Effects of aggregate bulking and film thicknesses on water permeability and strength of pervious concrete. *Powder Technology*, *396*, 743–753. https://doi.org/10.1016/J.POWTEC.2021.11.019

López, A., Tobes, J. M., Giaccio, G., & Zerbino, R. (2009). Advantages of mortar-based design for coloured self-compacting concrete. *Cement and Concrete Composites*, *31*(10), 754–761. https://doi.org/10.1016/J.CEMCONCOMP.2009.07.005

Lukovic, M., Ye, G., & Van Breugel, K. (2012). Reliable concrete repair: A critical review. *14th International Conference Structural Faults and Repair*, *Edinburgh, Scotland, UK*. October 2015. https://repository.tudelft.nl/islandora/object/uuid:0bb2bee0-027c-4384-a1fc-c995c9bba1c0.

Luo, Q., Wang, W., Wang, B., Xu, S., & Sun, Z. (2021). Numerical study on interface optimization of new-to-old concrete with the slant grooves. *Structures*, *34*, 381–399. https://doi.org/10.1016/J.ISTRUC.2021.07.094

Mansour, W., & Fayed, S. (2021). Effect of interfacial surface preparation technique on bond characteristics of both NSC-UHPFRC and NSC-NSC composites. *Structures*, *29*, 147–166. https://doi.org/10.1016/J.ISTRUC.2020.11.010

Milovancevic, M., Denić, N., Ćirković, B., Nešić, Z., Paunović, M., & Stojanović, J. (2021). Prediction of shear debonding strength of concrete structure with high-performance fiber reinforced concrete. *Structures*, *33*, 4475–4480. https://doi.org/10.1016/J.ISTRUC.2021.07.012

Mohamed, O., Kewalramani, M., Ati, M., & Hawat, W. A. (2021). Application of ANN for prediction of chloride penetration resistance and concrete compressive strength. *Materialia*, *17*, 101123. https://doi.org/10.1016/J.MTLA.2021.101123

Momayez, A., Ehsani, M. R., Ramezanianpour, A. A., & Rajaie, H. (2005). Comparison of methods for evaluating bond strength between concrete substrate and repair materials. *Cement and Concrete Research*, *35*(4), 748–757. https://doi.org/10.1016/j.cemconres.2004.05.027

Morgan, D. R. (1996). Compatibility of concrete repair materials and systems. *Construction and Building Materials*, *10*(1), 57–67. SPEC. ISS. https://doi.org/10.1016/0950-0618(95)00060-7

Mu, B., Meyer, C., & Shimanovich, S. (2002). Improving the interface bond between fiber mesh and cementitious matrix. *Cement and Concrete Research*, *32*(5), 783–787. https://doi.org/10.1016/S0008-8846(02)00715-9

Muthupriya, P., Subramanian, K., & Vishnuram, B. G. (2011). Prediction of compressive strength and durability of high performance concrete by artificial neural networks. *International Journal of Optimization in Civil Engineering*, *1*(1), 189–209. http://ijoce.iust.ac.ir/browse.php?a_code=A-10-1-12&slc_lang=en&sid=1

Naderi, M., & Ghodousian, O. (2012). Adhesion of self-compacting overlays applied to different concrete substrates and its prediction by fuzzy logic. *The Journal of Adhesion*, *88*(10), 848–865. https://doi.org/10.1080/00218464.2012.705673

Naderi, M., Qodousian, O., & Dehshali, H. M. (2012). Effects of type and dosage of pigment on the concrete compressive strength and its prediction by the fuzzy logic. *Journal of Color Science and Technology*, *5*(3), 315–324.

Öztaş, A., Pala, M., Özbay, E., Kanca, E., Çagˇlar, N., & Bhatti, M. A. (2006). Predicting the compressive strength and slump of high strength concrete using neural network. *Construction and Building Materials*, *20*(9), 769–775. https://doi.org/10.1016/j.conbuildmat.2005.01.054

Qian, J., You, C., Wang, Q., Wang, H., & Jia, X. (2014). A method for assessing bond performance of cement-based repair materials. *Construction and Building Materials*, *68*, 307–313. https://doi.org/10.1016/j.conbuildmat.2014.06.048

Qiu, J., Guo, Z., Yang, L., Jiang, H., & Zhao, Y. (2020). Effects of packing density and water film thickness on the fluidity behaviour of cemented paste backfill. *Powder Technology*, *359*, 27–35. https://doi.org/10.1016/J.POWTEC.2019.10.046

Rashid, K., Ahmad, M., Ueda, T., Deng, J., Aslam, K., Nazir, I., & Azam Sarwar, M. (2020). Experimental investigation of the bond strength between new to old concrete using different adhesive layers. *Construction and Building Materials*, *249*, 118798. https://doi.org/10.1016/J.CONBUILDMAT.2020.118798

Sharma, K. K., Imam, A., Anifowose, F., & Srivastava, V. (2020). Compressive strength modeling of blended concrete based on empirical and artificial neural network techniques. *Journal of Structural Integrity and Maintenance*, *5*(4), 252–264. https://doi.org/10.1080/24705314.2020.1783120

Wang, B., Xu, S., & Liu, F. (2016). Evaluation of tensile bonding strength between UHTCC repair materials and concrete substrate. *Construction and Building Materials*, *112*, 595–606. https://doi.org/10.1016/j.conbuildmat.2016.02.149

Zanotti, C., Rostagno, G., & Tingley, B. (2018). Further evidence of interfacial adhesive bond strength enhancement through fiber reinforcement in repairs. *Construction and Building Materials*, *160*, 775–785. https://doi.org/10.1016/j.conbuildmat.2017.12.140

Zarandi, M. F., Türksen, I. B., Sobhani, J., & Ramezanianpour, A. A. (2008). Fuzzy polynomial neural networks for approximation of the compressive strength of concrete. *Applied Soft Computing Journal*, *8*(1), 488–498. https://doi.org/10.1016/j.asoc.2007.02.010

Zurita Ares, M. C., Villa González, E., Torres Gómez, A. I., & Fernández, J. M. (2014). An easy method to estimate the concentration of mineral pigments in colored mortars. *Dyes and Pigments*, *101*, 329–337. https://doi.org/10.1016/J.DYEPIG.2013.10.001

Appendix

Appendix A

This section presents details of a Generalised Nearest Neighbourhood Clustering (GNNC) method used to predict the interfacial bond strength of the specimens. A modified Particle Swarm Optimisation (PSO) algorithm was used to optimise the parameters of the fuzzy system by movements in a search space including both continuous and integer variables. In the modified PSO, each particle alters not only the optimal fuzzy system by adjusting the parameters $\sigma_1, \sigma_2, \ldots, \sigma_n$, but also the GNNC through adjusting the radius r. In this study, each particle is represented as follows:

$$X_p = [\sigma_{p1}, \sigma_{p_2}, \ldots, \sigma_{p_n}, r_p] \tag{2}$$

where $\sigma_{p_1}, \sigma_{p_2}, \ldots, \sigma_{pn}$ and r_p are parameters and radius projected by particle X_p to modify the subsequent fuzzy system. In summary, every particle $X_p (p = 1, 2, \ldots, N)$ provides a radius, r_p by which a GNNC is developed. At that point, by utilising the resulting clusters and the parameters $\sigma_{p1}, \sigma_{p2}, \ldots, \sigma_{pn}$ of X_p, the fuzzy system related to X_p is formulated as:

$$f_p(x) = \frac{\sum_{l=1}^{M_p} Y^l \left[\prod_{i=1}^{n} \exp\left(-\left(\frac{x_i - (x_{cp}^l)_i}{\sigma_{pi}}\right)^2\right)\right]}{\sum_{l=1}^{M_p} N^l \left[\prod_{i=1}^{n} \exp\left(-\left(\frac{x_i - (x_{cp}^l)_i}{\sigma_{pi}}\right)^2\right)\right]} \tag{3}$$

where M_p is the quantity of clusters and X_{cp}^1 $(l = 1, 2, \ldots, M_p)$ are cluster centres resulting from the particle X_p.

Objective function

Consider the p'th particle X_p and its associated optimal fuzzy system $f_p(x)$. In addition, assume that $\varepsilon > 0$ and M input-output pairs (x^1, y^1), $l = 1, 2, \ldots, M$, are provided. The objective function which was minimised by the algorithm is:

$$f(X_p) = \max\left\{\varepsilon, \max_{l=1}^{M}\{\, |f_p(x^l) - y^l| \,\}\right\} \tag{4}$$

Updating particle's positions and velocities

The first variables of $X_p = [\sigma_{p1}, \sigma_{p2}, \ldots, \sigma_{pn}, r_p]$ and V_p $(p = 1, 2, \ldots, N)$ are updated by Equation (5). In this case, $r_p \in \{d_0, 2d_0, \ldots, Rd_0\}$ is considered as an assumption in which R is a pre-specified integer number, and d_0 is selected as the minimum distance between the inputs of training data. This is based on the fact that different values of radius r_p may often lead to the same clusters (notably, those values that are too neighbouring). Thus, considering a continuous range for a variable r_p may be considerably more time and energy-consuming. In consequence, the $(n+1)$'th variable of X_p and V_p are updated and modified as follows:

$$\begin{aligned}(V_p)_{n+1}(t+1) &= max\left\{(V_p)_{n+1}(t), (X_p)_{n+1}(t), (P_p)_{n+1}, (P*)_{n+1}\right\}(X_p)_{n+1}(t+1) \\ &= \left[\frac{(X_p)_{n+1}(t) + (V_p)_{n+1}(t+1)}{2}\right]\end{aligned} \tag{5}$$

where $(X_p)_{n+1}$, $(V_p)_{n+1}$, $(p_p)_{n+1}$ and $(P^*)_{n+1}$ are the $(n+1)$'th component of vectors X_p, V_p, P_p and P^*, respectively. Furthermore, $[z]$ is the highest integer less than or equal to z.